

## Supplementary Information

### **Tetrahydromagnolol induces autophagic cell death by targeting the m<sup>6</sup>A reader protein YTHDF2 and enhances the efficacy of anti-PD-1 immunotherapy in pancreatic cancer cells**

Guohua Li<sup>1, 2, #</sup>, Qibiao Wu<sup>2, #</sup>, Yiping Mou<sup>3, #</sup> Yunhao Qiao<sup>1, #</sup>, Lijun Jin<sup>4</sup>, Qian Shi<sup>1</sup>, Ruonan Zhang<sup>1</sup>, Jie Li<sup>1, 2</sup>, Yitian Sun<sup>1, 2</sup>, Aili Zhang<sup>1, 2</sup>, Haiyang Jiang<sup>1</sup>, Zijing Yang<sup>1</sup>, Zhiyu Zhu<sup>1</sup>, Mengmeng Ma<sup>1</sup>, Xiaoyu Sun<sup>1</sup>, Xinbing Sui<sup>1, 2,\*</sup>

<sup>1</sup> School of Pharmacy, Hangzhou Normal University, Hangzhou, 311121, Zhejiang, China

<sup>2</sup> State Key Laboratory of Quality Research in Chinese Medicines, Faculty of Chinese Medicine, Macau University of Science and Technology, Macau, P.R. China

<sup>3</sup> Department of Gastrointestinal and Pancreatic Surgery, Zhejiang Provincial People's Hospital, People's Hospital of Hangzhou Medical College, Hangzhou, Zhejiang, China

<sup>4</sup> Department of Traditional Chinese Medicine, The Second Affiliated Hospital, School of Medicine, Zhejiang University, Hangzhou, Zhejiang, China

\*Correspondence: suilab@hznu.edu.cn (X.S.)

#These authors contribute equally.

## Supplementary Figures:

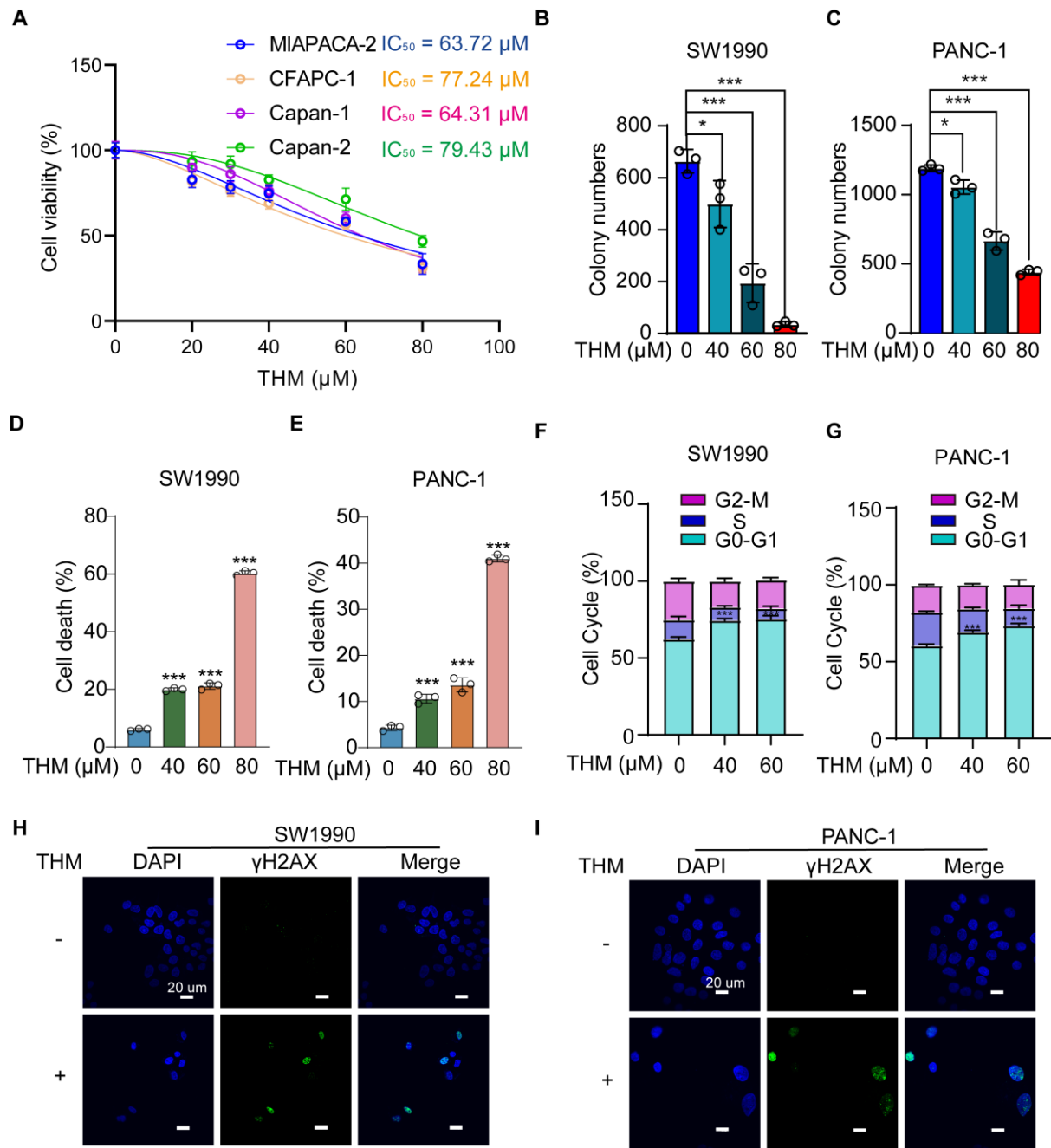


**Figure S1.** THM inhibited cell proliferation and induced cell death in pancreatic cancer cells. **(A)** MIAPaCa-2, CFAPC-1, Capan1 and Capan2 cells were treated with different concentrations of THM for 24 h, and cell viability was measured by CCK8 assay. **(B-C)** The quantitative analysis of the colony formation after the treatment with THM, means  $\pm$ S.D., n = 3; \* $p$  < 0.05, \*\*\* $p$  < 0.001. **(D-E)** The quantitative analysis of annexin V-FITC/ PI staining after the treatment with THM for 24 h, means  $\pm$ S.D., n = 3; \*\* $p$  < 0.01, \*\*\* $p$  < 0.001. **(F-G)** The quantitative analysis of cell cycle after the treatment with THM for 24 h. **(H-I)** Immunofluorescence staining for DNA damage marker  $\gamma$ -H2AX in SW1990 and PANC-1 cells after THM treatment for 24 h.

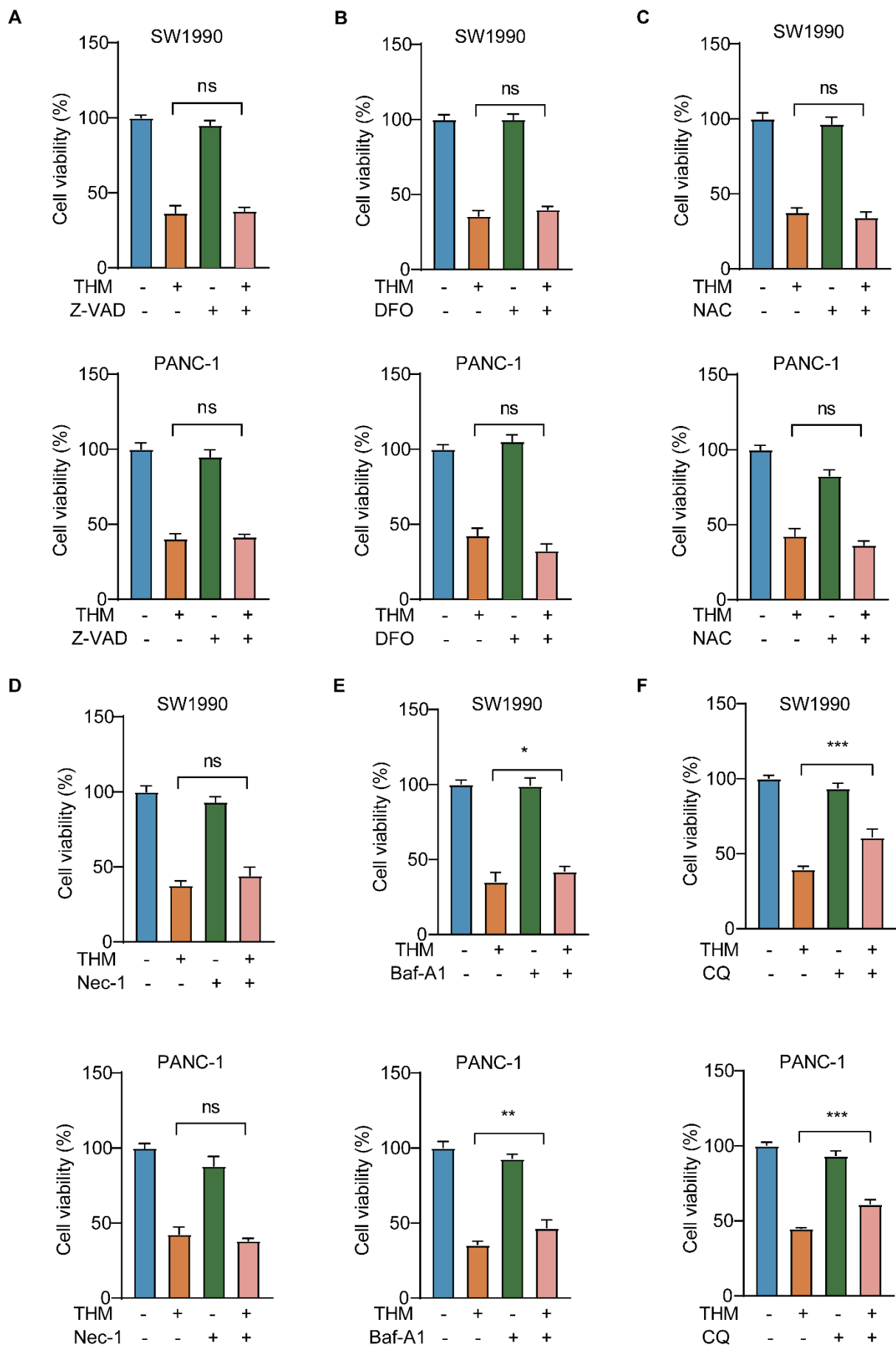


**Figure S2.** The effect of THM alone or combines with different cell death inhibitors on the cell viability of pancreatic cancer cells. **(A)** SW1990 and PANC-1 cells were treated with THM with or without Z-VAD (10  $\mu$ M) for 24 h, and cell viability was detected. **(B)** SW1990 and PANC-1 cells were treated with THM with or without DFO (10  $\mu$ M) for 24 h, and cell viability was detected. **(C)** SW1990 and PANC-1 cells were treated with THM with or without NAC (1 mM) for 24 h, and cell viability was detected. **(D)** SW1990 and PANC-1 cells were treated with THM with or without Nec-1 (10  $\mu$ M) for 24 h, and cell viability was detected. **(E)** SW1990 and PANC-1 cells were treated with THM with or without Baf-A1 (20 nM) for 24 h, and cell viability was detected. **(F)** SW1990 and PANC-1 cells were treated with THM with or without CQ (25  $\mu$ M) for 24 h, and cell viability was detected. Data are summarized as mean  $\pm$  S.D., \* $p$  < 0.05, \*\* $p$  < 0.01, \*\*\* $p$  < 0.001, ns: not significant (n = 3).

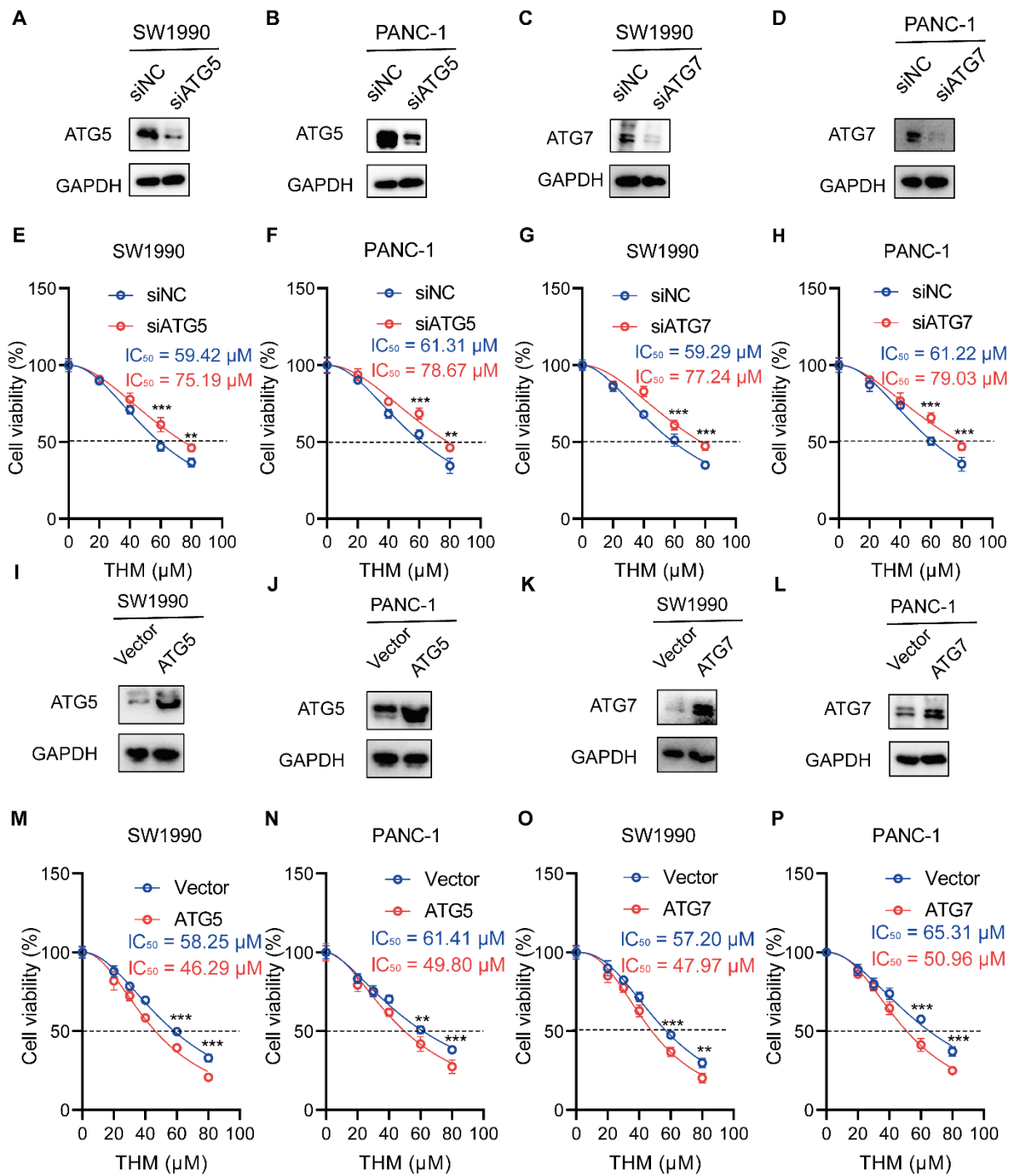


**Figure S3.** THM affected the cytotoxicity of pancreatic cancer cells through autophagy-related proteins ATG5 and ATG7 **(A-D)** ATG5/7 proteins in knocked-down SW1990 and PANC-1 cells were analyzed by western blot. GAPDH was used as internal control. **(E-H)** SW1990 and PANC-1 cells were treated with different concentrations of THM for 24 h after knocking down the expression of ATG5/7, and cell viability was measured by CCK8 assay. n = 3; \*\*p < 0.01, \*\*\*p < 0.001. **(I-L)** ATG5/7 proteins in over-expressed SW1990 and PANC-1 cells were analyzed by western blot. GAPDH was used as internal control. **(M-P)** SW1990 and PANC-1 cells were treated with different concentrations of THM for 24 h after overexpression of ATG5/7, and cell viability was measured by CCK8 assay. n = 3; \*\*p < 0.01, \*\*\*p < 0.001.

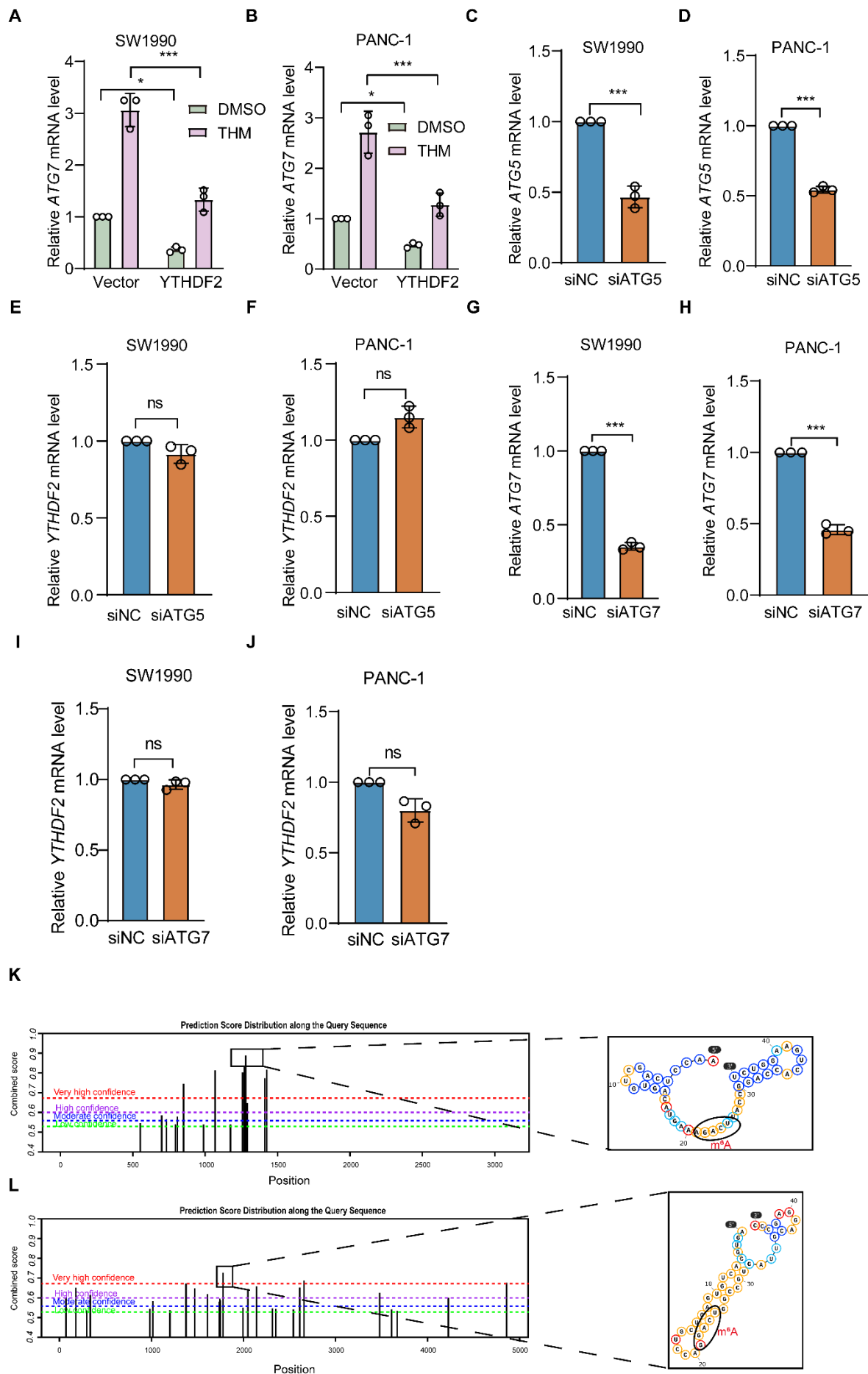


**Figure S4.** THM suppressed YTHDF2 recognition of m<sup>6</sup>A mRNA targets. **(A-B)** Analysis of ATG7 mRNA expression in SW1990 and PANC-1 cells by RT-qPCR after overexpression of YTHDF2 with or without THM treatment. n = 3; \*\*\*p < 0.001. **(C-F)** Analysis of ATG5 and YTHDF2 mRNA expression in SW1990 and PANC-1 cells by RT-qPCR after knockdown of ATG5. n = 3; \*\*p < 0.01. **(G-J)** Analysis of ATG7 and YTHDF2 mRNA expression in SW1990 and PANC-1 cells by RT-qPCR after knockdown of ATG7. n = 3; \*\*p < 0.01. **(K-L)** The predicted m<sup>6</sup>A sites of ATG5 and ATG7 mRNA via SRAMP (<http://www.cuilab.cn/sramp/>).

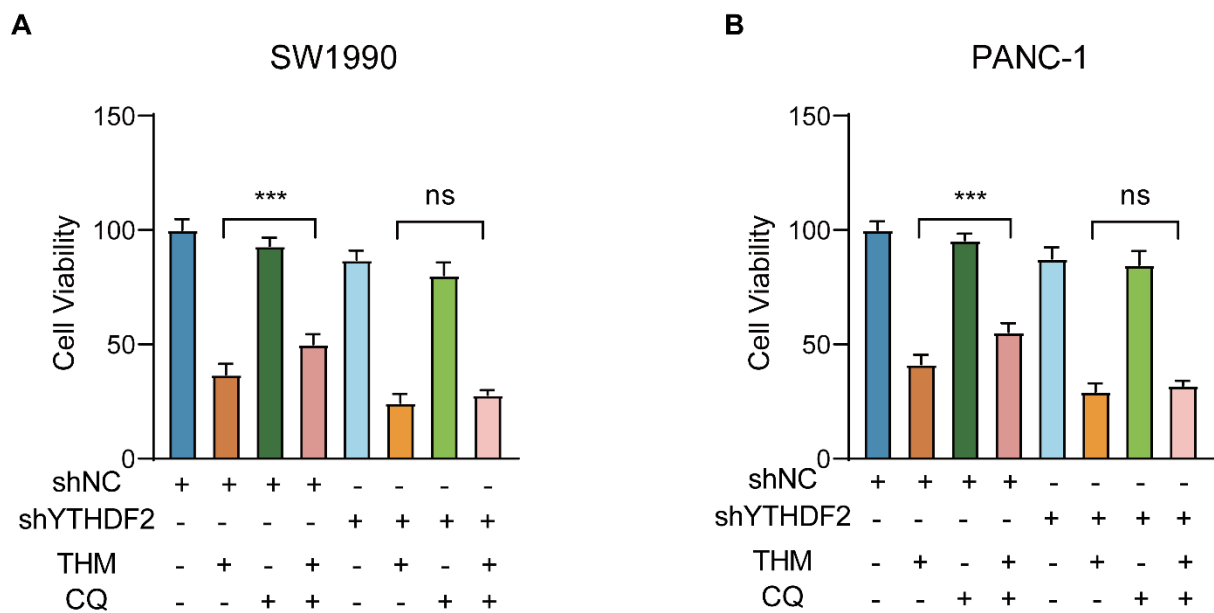


**Figure S5.** Effects of THM on cell viability through YTHDF2 and autophagy regulation in pancreatic cancer cells. **(A-B)** Analysis of cell viability in SW1990 and PANC-1 cells by CCK8 assay after transfection with shNC or shYTHDF2 and treatment with THM with or without CQ for 24 h. Data are presented as mean  $\pm$  S.D. of three independent experiments. \*\*\* $p < 0.001$ , ns: not significant.

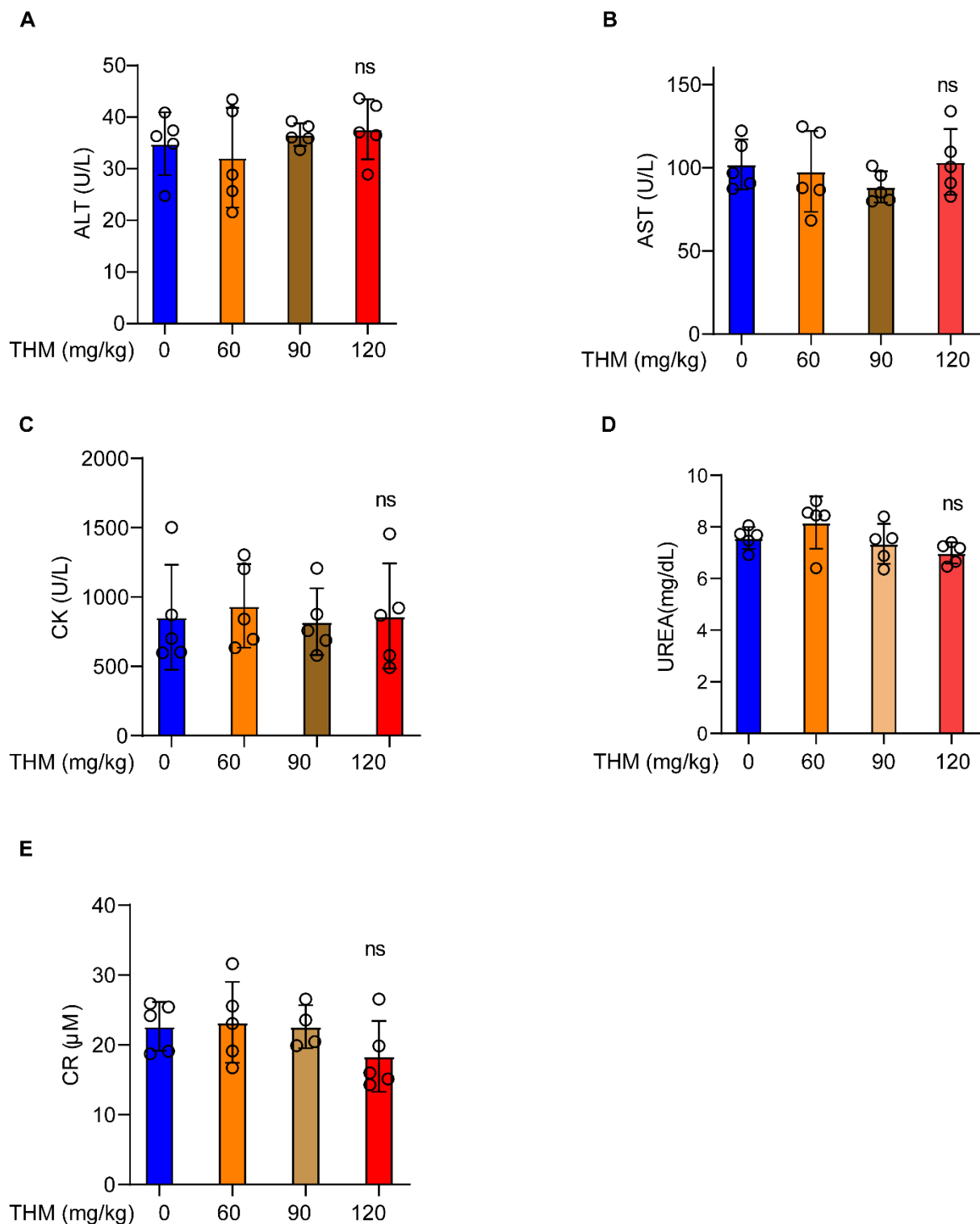


**Figure S6.** Safety evaluation of THM on pancreatic cancer was evaluated in xenograft models *in vivo*. **(A)** After treatment with saline or THM for 10 times, mice serum was taken for the determination of alanine transaminase (ALT) assay. **(B)** After treatment with saline or THM for 10 times, mice serum was taken for aspartate aminotransferase (AST) assay. **(C)** After treatment with saline or THM for 10 times, mice serum was taken for creatine kinase (CK) assay. **(D)** After treatment with saline or THM for 10 times, mice serum was taken for urea (UREA) assay. **(E)** After treatment with saline or THM for 10 times, mice serum was taken for

creatinine (CR) assay. All the data are presented as means  $\pm$ S.D. ns: there was no significant difference.

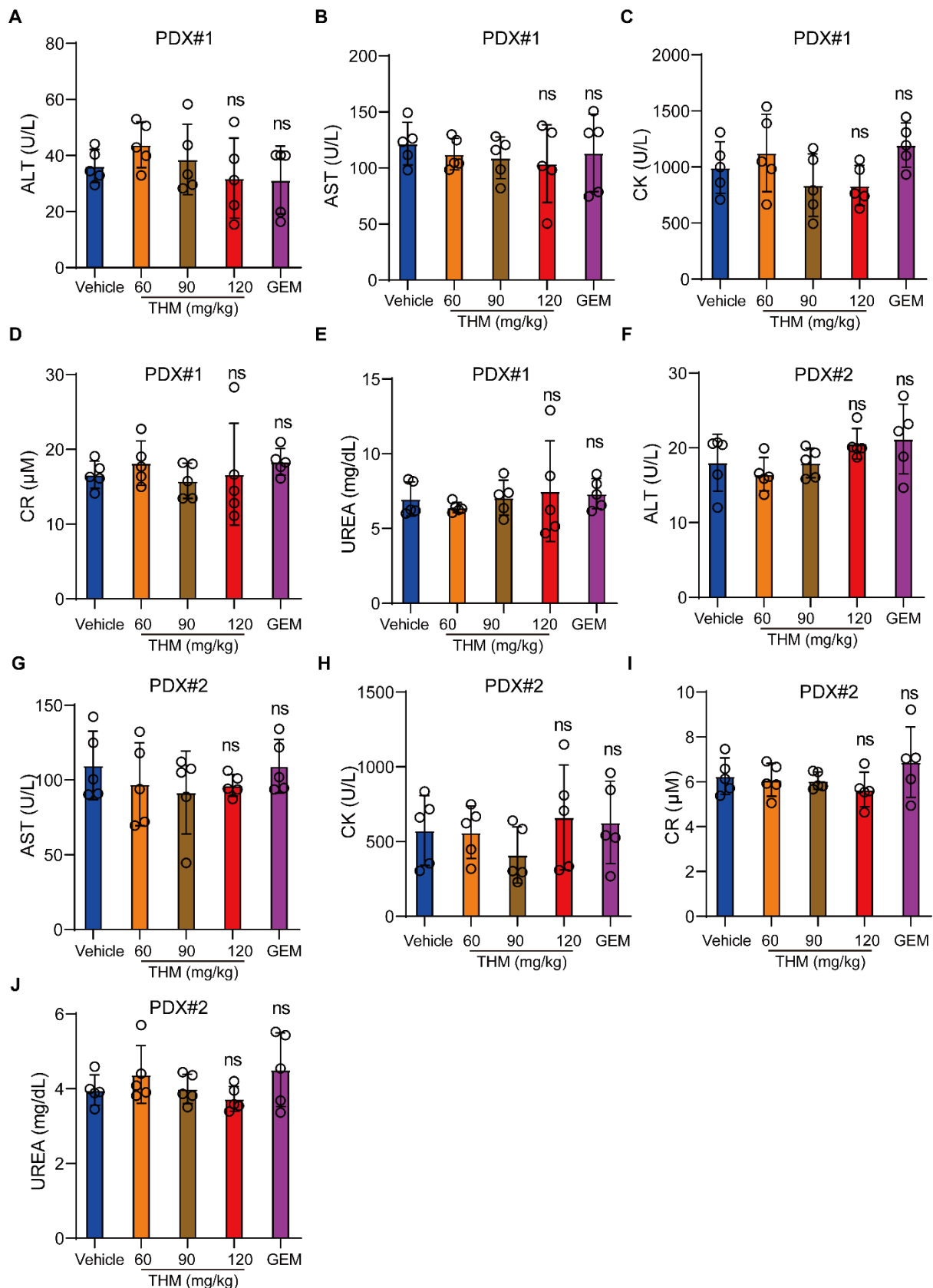


**Figure S7.** Safety evaluation of THM on pancreatic cancer was evaluated in PDX models *in vivo*. **(A)** PDX#1 mice serum was taken for the determination of ALT assay in different groups. **(B)** PDX#1 mice serum was taken for AST assay in different groups. **(C)** PDX#1 mice serum

was taken for CK assay in different groups. **(D)** PDX#1 mice serum was taken for CR assay in different groups. **(E)** PDX#1 mice serum was taken for UREA assay in different groups. **(F)** PDX#2 mice serum was taken for the determination of ALT assay in different groups. **(G)** PDX#2 mice serum was taken for aspartate aminotransferase (AST) assay in different groups. **(H)** PDX#2 mice serum was taken for CK assay in different groups. **(I)** PDX#2 mice serum was taken for CR assay in different groups. **(J)** PDX#2 mice serum was taken for UREA assay in different groups. All the data are presented as means  $\pm$ S.D. ns: there was no significant difference.

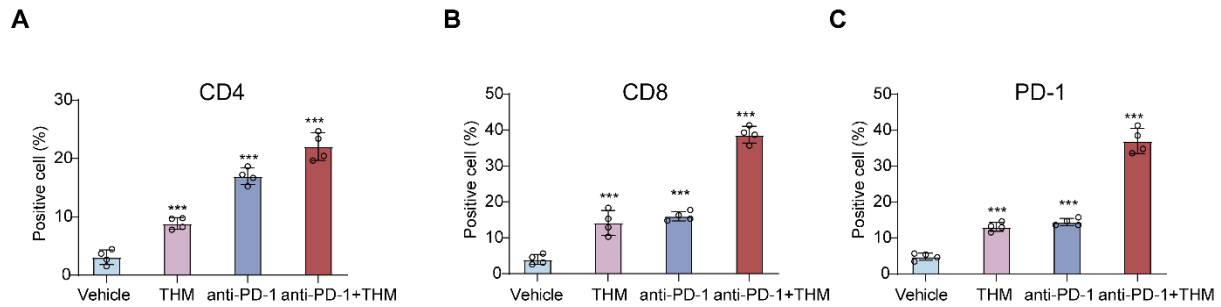


**Figure S8.** Effects of THM and anti-PD-1 combination therapy on immune infiltration in pancreatic cancer. **(A-C)** Quantitative analysis of immunohistochemical staining for CD4, CD8a and PD-1 in orthotopic Pan02-Luc pancreatic cancer tumor sections. Data are summarized as mean  $\pm$  S.D., \*\*\* $p$  < 0.001, ns: not significant ( $n$  = 4).

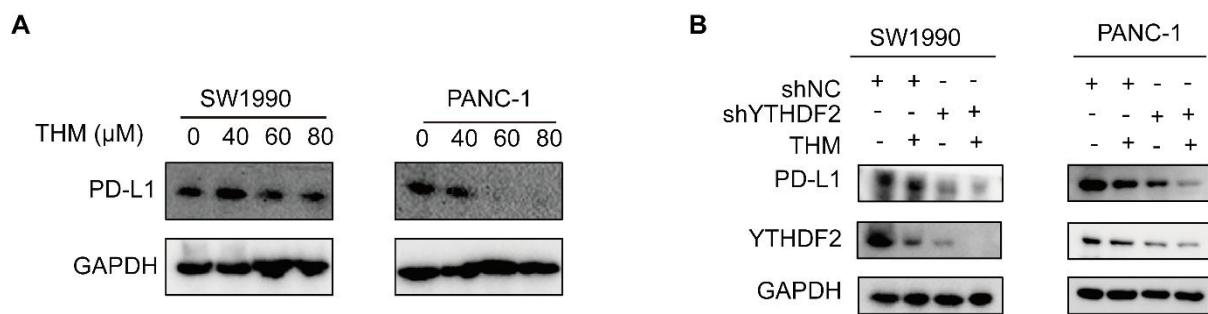


**Figure S9.** Effects of THM on PD-L1 expression in pancreatic cancer cells *via* the YTHDF2 signaling pathway. **(A)** SW1990 and PANC-1 cells were treated with different concentrations of THM for 24 h, and PD-L1 protein levels were detected by western blot. **(B)** SW1990 and PANC-1 cells with stable shNC or shYTHDF2 were treated with THM for 24 h, and PD-L1 and YTHDF2 protein levels were detected by western blot.